ELSEVIER

Contents lists available at ScienceDirect

Forest Ecology and Management

journal homepage: www.elsevier.com/locate/foreco





War threatens 18 % of protective plantations in eastern agroforestry region of Ukraine

Maksym Matsala a,*, Andrii Odruzhenko b, Serhii Sydorenko c, Svitlana Sydorenko d,e

- ^a Swedish University of Agricultural Sciences, Southern Swedish Forest Research Centre, Sundsvägen 3, Alnarp 23456, Sweden
- ^b National University of Life and Environmental Sciences of Ukraine, Heroiv Oborony St. 15, Kyiv 03041, Ukraine
- ^c Wageningen University, Droevendaalsesteeg 3, Wageningen 6708, the Netherlands
- d Ukrainian Order 'Sign of Honour' Research Institute of Forestry and Forest Melioration named after G. M. Vysotsky, Hryhoriia Skovorody St. 86, Kharkiv 61024, Ukraine
- ^e Ukrainian Research Institute of Forestry and Forest Melioration, Kharkiv 61024, Ukraine

ARTICLE INFO

Keywords: Shelterbelts Windbreaks Environmental damage Forest degradation Remote sensing

ABSTRACT

The ongoing Russian invasion in Ukraine has significantly impacted the forest ecosystems at national scale, including the crucial agroforestry systems in the eastern part of country. This study focuses on estimating the damage caused to forest protective plantations in 2022-2023, with particular focus on the loss of cropland protection function derived by shelterbelts. We used a soil type map and damaged forest cover estimates to report the areas of expected post-war regeneration options by tree species, both native and alien. We applied satellite remote sensing data and raster patch analysis to semi-automatically classify a forest cover mask (as of 2021) on functional types: shelterbelts, urban forests, ravine protection, water protection, and roadside protective plantations. We revealed that 18 % of the protective plantations have been damaged as of 2023. Despite this extensive damage, the overall loss of cropland protection function across the study area was relatively modest, at 2.7 % as of 2023. However, localized hotspots exhibited losses up to 57 %, correlating with the proximity to main fights occurred in 2022-2023. We reported that the majority (81 %) of the damaged plantations are on fertile black earth soils, which favor the regeneration using a variety of native tree species. However, there are hitherto risks associated with the use of alien species, driven both by economic pressures and legislative ambiguities. Our study highlights the importance of satellite data analysis as a tool to report direct war impact on eastern agroforestry region of Ukraine. Simultaneously, we call for strategies to collect high-resolution data for spatial models' calibration and validation. We emphasize the necessity to consider spatial analysis for planning post-war forest regeneration efforts.

1. Introduction

As of the beginning of 2024, Ukraine has been under full-scale Russian military invasion for two years. Several research studies, technical reports, and media articles have revealed massive damage to agricultural systems (Kussul et al., 2024), forests (Matsala et al., 2024), freshwater systems (Gleick et al., 2023; Shumilova et al., 2023), and coastal ecosystems (Shevchuk et al., 2022). The full scale of associated degradation of ecosystem services and biodiversity loss cannot yet be accurately measured, due to the ongoing nature of military activities (Pereira et al., 2022; Rawtani et al., 2022).

Fires and mechanical pollution by unexploded ordnance (UXO) are considered the main factors negatively impacting war-affected

terrestrial ecosystems in Ukraine (Zibtsev et al., 2023). This damage threatens the sustainability of rural communities of the comparatively forest-poor southern and eastern regions of Ukraine (Shvidenko et al., 2017; Hall et al., 2021). First, landscape fires that follow shelling destroy shelterbelts (or windbreaks), important for sustaining an even snow cover over croplands (Vacek et al., 2018) or in plantations established to regulate soil erosion. Second, ignitions can contribute to soil erosion in human-modified landscapes (e.g., Depountis et al., 2020). Third, UXO contamination disrupts logistical and economic connections in agroforestry systems and threatens human security (Butsic et al., 2015).

However, efforts to map environmental damage have been focused on croplands (Kussul et al., 2024) or the region's largest forest massifs (Matsala et al., 2024) directly affected by military activities. But the vast

E-mail address: Maksym.matsala@slu.se (M. Matsala).

^{*} Corresponding author.

southern and eastern agricultural regions of Ukraine are characterized by scattered, highly fragmented tree cover in the form of small forest massifs, woodlands, and protective plantations (Myroniuk et al., 2020), and this fragmented spatial pattern, and their smaller absolute area compared to larger forest massifs have contributed to an insufficient research focus and mapping efforts. These protective plantations are of high importance for erosion control, cropland yield protection, and water regulation. They serve as natural buffers between industrial agglomerations (Sun et al., 2022) evenly distributed across the region.

Satellite imagery has been used to map conflict-associated forest cover loss or degradation for decades (Gorsevski et al., 2012; Butsic et al., 2015; Negash et al., 2023). It is a suitable reference tool due to the physical inaccessibility of vast areas still affected by ongoing battles or contaminated by UXO (Shumilo et al., 2024). As such, time series of satellite images can give cost-efficient and reliable data on protracted, indirect impacts of military conflicts on forest ecosystems (Dong et al., 2020). Satellite data are also frequently used to estimate ecosystem functions of agroforestry systems, mainly through assessing the structural parameters of shelterbelts (Yang et al., 2021, Deng et al., 2023). While some of these parameters can be preferably estimated by acquiring airborne laser scanning data (Nowak et al., 2022), this option is not possible in Ukraine, as no aircraft can fly close to the conflict-affected zone.

Maps of the detected damaged forest cover after stratification by soil types, topography, and climatic regimes can be used to plan post-war ecosystem regeneration. Native species are the optimal solution if growth conditions favor their application (Stadnik, 2018; Dubyna et al., 2023). However, droughts and economic pressure on human-modified landscapes can threaten traditional pathways for restoring degraded shelterbelts and other protective plantations. The risk of applying 'traditional' (such as black locust, *Robinia pseudoacacia*) and new (e.g., green ash, *Fraxinus pensylvanica*) alien species with the aim to reduce the cost of forest restoration will likely be high.

This study estimated the damage to forest ecosystems in the eastern region of Ukraine, along the frontline. We focused on agroforestry-related, erosion control, and societally important (e.g., urban) forest types and excluded large production or protected forests along the Siverskyi Donets River. We used openly available geospatial products to classify forest cover into functional types and then estimated the damage that occurred in 2022 and 2023. We hypothesize (H1) that the area of damaged forest cover has increased up to 2023, indicating the further deterioration of environmental condition caused by Russia's invasion. Also, we estimated the war-related change to the cropland protection function provided by shelterbelts. Based on our media monitoring, we thus expect a large decrease (H2) in this ecosystem function at the study area level due to alleged destruction of shelterbelts.

Additionally, we used a soil map to understand which native and, in some cases, alien tree and shrub species can be used to restore protective plantations in the study area. In this way, we initiate discussion of the potential to sustainably regenerate degraded forests in the eastern agroforestry region of Ukraine.

2. Methods and materials

2.1. Study area

Selected administrative counties ('hromadas') belong to the forest-steppe biogeographical region (north to Siverskyi Donets River) or steppe zone (south to Siverskyi Donets River). The topography is plain (average elevation is 144 m above sea level according to Shuttle Radar Topography Mission, 2000). Soils are dominated by rich and fertile black soils, which define the agricultural importance of this area. Croplands are the main land use in study area, while forest massifs can be attributed to basins of Siverskyi Donets and Oskil Rivers. Forests are dominated by planted Scots pine (*Pinus sylvestris* L.). Wetter sites, mostly along the Siverskyi Donets River, are covered by deciduous forests

(represented by, e.g., European oak, *Quercus robur* L. or black alder, *Alnus glutinosa* (Gaertn.) L.). Grasslands (pastures, meadows, natural steppe remnants in protected areas) occur along the smaller rivers and in ravines. The climate is dry continental, with average annual precipitation ranging from 400 (in the southern part of study area) to 500 (in the northern part) mm. The average temperature in July is $+21\,^{\circ}\text{C}$ and $-7\,^{\circ}\text{C}$ in January. The leaf-on season lasts for 190 ± 5 days, with a total of 280 mm of precipitation on average (Soshenskyi et al., 2022).

2.2. Land cover and damaged forest cover classification

We used classification models developed for the east of Ukraine in Matsala et al. (2024). The land cover classification model was Random Forest (RF) trained on manually interpreted samples and both optical (Sentinel-2) and radar (Sentinel-1) satellite imagery at 10 m spatial resolution. The overall accuracy for this model was 81.6 %, with the user's accuracy for class 'forest cover' at 79.2 %. The damaged forest cover model was a binary RF classifier trained on the sample of high-resolution satellite images and their visual interpretation. The spectral difference (delta) between two July–September median values (for 2021 and 2022) of Sentinel-2 bands and vegetation indices (Normalized Burn Ratio and Normalized Difference Vegetation Index) were used to calibrate this classifier. The overall accuracy of the RF model of damaged forest cover was 95.8 %.

First, we extracted forest cover (dense tree cover, ignoring the 'shrublands' class, which may contain young forests) from a land cover map predicted for the year 2021. Second, we separately predicted damaged forest cover within this mask based on a spectral change between 2021 and 2022, and between 2021 and 2023 (H1). We extracted satellite data using Google Earth Engine (Gorelick et al., 2017) and processed it in R.

2.3. Forest functional types

We created a rule-based classification map of forest functional types (Table 1) for 2021 in a rapid and semi-automated way. First, we set aside tree cover within the administrative boundaries of settlements using official vector layers (Fig. 2). This functional type was considered as 'urban forests' (Forest Code, 2006), even though some shelterbelts, ravine protection, and other forests were also located within the boundaries of villages, towns, and cities. Second, we manually excluded large forest massifs along the Siverskyi Donets River and Oskil River. Though these forests are crucial for the eastern region of Ukraine as a source of diverse ecosystem services, their large area (and reported damages, Matsala et al., 2024) would bias our analysis towards timber supply, not agroforestry and community-related dimensions.

Third, we extracted pixels of the remaining forest cover mask within the buffer zones of rivers, water bodies, highways, and railroads. We used adjusted Open Street Map layers: minor streams were filtered out from the river layer and additional roads were digitized if missing. In line with Ukrainian regulations, 50 m buffers were delineated around rivers, highways, and railroads, while 00 m zones were created around water bodies, such as lakes and reservoirs. We considered pixels within these buffer zones as 'water protection plantations' and 'roadside protective plantations', respectively.

Fourth, we attempted to detect 'ravine protection' forests using specific topography features. We used a product, Global ALOS Landforms, a raster map at 90 m spatial resolution, which depicts peaks, ridges, valleys, and slopes based on a digital surface model. We resampled this layer to a 10 m spatial resolution and extracted pixels with values corresponding to 'lower slope', 'lower slope (warm)', 'valley', and 'valley (narrow)'. We considered these landform classes as able to best represent ravines in our study area.

Fifth, for the remaining forest mask, we calculated synthetic layers of patch characteristics using the R library 'landscapemetrics'. We mapped layers of calculated perimeter-area ratio, patch area, and patch core area

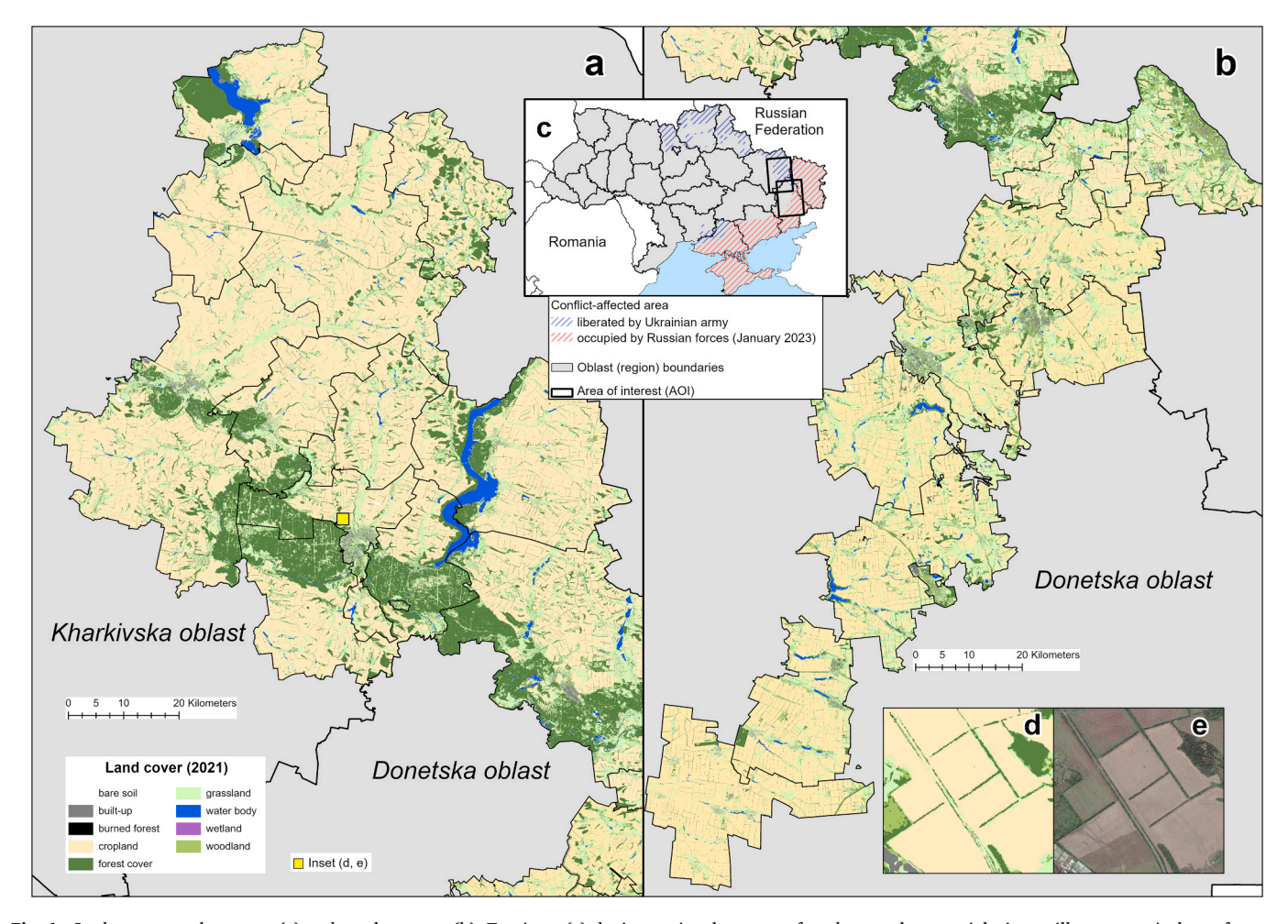


Fig. 1. Study area: northern part (a) and southern part (b). Top inset (c) depicts national context of study area, bottom right insets illustrate typical agroforestry system with predicted land cover (d) and World-View 3 satellite image (e) acquired in August 2022.

index. Patch area is the area of pixels connected in eight directions and belonging to one class. Patch perimeter-area ratio reflects patch shape complexity, i.e. patches with longer perimeters and more edges. The patch core area index shows the percentage of patch area, which is core area, i.e. area of pixels not belonging to patch edges. We visually explored these values in the GIS environment to understand which thresholds are most feasible for capturing the linear and narrow shape of 'shelterbelts'. Pixels were considered part of a shelterbelt if they had perimeter-area ratio >0.07, and patch area of at least 0.3 ha. Next, we considered remaining pixels with perimeter-area ratio between 0.04 and 0.07, applying the filter of core area index >22. For the remaining pixels with core area index >70 and perimeter-area ratio <0.04 we also considered functional type 'shelterbelts'.

Sixth, if remaining patches of pixels were within 10 or 20 m of Euclidean distance to the already created 'ravine protection plantations' mask or the 'other forests' type, they were added to the 'ravine forests' type layer.

We constructed a random stratification scheme of independent validation 'plots': 400 points for each forest functional type (allocated within the final raster layer), except 'urban forests'. In total, we interpreted 2000 points in the Collect Earth environment (Bey et al., 2016) using visual inspection of high-resolution satellite data to assign 'ground-truth' forest functional type.

We reported area estimates for each forest functional type and their damage level using established protocol (Olofsson et al., 2014). We propagated area estimate uncertainties by summarizing relative errors defined by confidence intervals (CI) of 'forest cover' class in land cover

model (Matsala et al., 2024, \pm 5.4 %), class 'damaged forest cover' in binary model (Matsala et al., 2024, \pm 14.4 %), and separately for every functional type (except for 'urban forests', where only errors related to land cover and damaged forest cover models were considered).

2.4. Degradation of cropland protection function

Based on visual analysis of Planet multispectral imagery (3 m spatial resolution) and observed spectral Sentinel-2 changes, we applied the threshold of 0.26 for Normalized Burn Ratio delta within the masks of forest cover damaged in 2022 and 2023. If delta values were below 0.26, the damage was considered 'low-medium'. This spectral change typically corresponded to low-severity fires following shelling, selective tree harvest, or mechanical tree damage with fast spectral recovery. If delta values were above 0.26, the damage was considered 'medium-high'. This category was characterized visually by total destruction of tree cover or medium or high-severity fires.

We calculated the change in cropland protection function caused by war-related damage (H2). First, we created a vector layer of single shelterbelts. For that, we vectorized raster patches of the 'shelterbelts' functional type mask as of the year 2021. Second, we calculated the width and length of each shelterbelt using ArcGIS Pro geometry instruments. Third, we predicted the mean height of each shelterbelt using a simple RF regression model. This model was trained using Sentinel-1 and Sentinel-2 median values from the leaf-on season (April – September 2021) as predictors, and GEDI-derived canopy height (at the 95th percentile). Canopy height 25 ×25 m pixels were vectorized and

Table 1
The definition of forest types.

Forest type	Description
Roadside protective plantations	Linear plantations of trees or shrubs are established along highways and railroads to protect roads from wind, snow, and erosion, to improve safety by reducing snowdrifts and dust, and to enhance the landscape. These plantations typically do not exceed a width of 100 m.
Ravine protection plantations	Forest plantations are created on ravines, sands, and reclaimed lands, and aimed at preventing soil erosion, stabilizing slopes, and rehabilitating degraded lands. These plantations enhance soil stability and improve water retention in vulnerable landscapes.
Shelterbelts	Protective linear tree plantations are established between agricultural fields to reduce wind speed, prevent soil erosion, and create a more favorable microclimate for crops. Shelterbelts also serve as barriers against pests and enhance biodiversity by providing habitats for various species.
Water protection plantations	Protective plantations consist of trees, shrubs, and grasses, and are strategically located along the shores of inland water bodies like lakes, ponds, and rivers. These green barriers serve as natural filters, safeguarding water quality by trapping pollutants from surface runoff. Furthermore, they are essential for stabilizing soil, preventing erosion, and nurturing diverse wildlife habitats.
Urban forests	Tree cover within urban areas, including parks, forest parks, and gardens. These forests improve air quality, provide recreational spaces, reduce urban heat islands, and enhance the aesthetic value of urban landscapes.
Other (unclassified) forests	Managed and protected forests, production tree plantations.

then we extracted mean values of Sentinel-1 or Sentinel-2 predictors within these square polygons, also weighing for the proportion of pixels within the square. Non-forest pixels and GEDI canopy height values below 5 m were excluded from the training data set. The height was then predicted for the 'shelterbelts' mask, and mean values were extracted for the shelterbelt polygons.

We used empirical knowledge from previous local research (Sydorenko and Sydorenko, 2018; Sydorenko et al., 2021) to derive a specific coefficient (0.46) to convert the width of the shelterbelt polygon to the 'practical' shelterbelt width. This calculation relies on the fact that remote sensing data maps the width of canopy cover, while the 'practical' width depicts the distance between the planted tree stems, and then is used in calculating cropland protection function. This was calculated using the function:

$$Fprot = L \times (D \times K \times H) / W$$
 (1)

where L is cropland-protective forest cover (%); D is n-distance (where n is equal to H in the formula) of efficient field protection; K is the average coefficient for shelterbelt aerodynamic design (dense - 0.7, sieve-looking - 0.8, blown - 1.0); H is the mean shelterbelt height, m; W is shelterbelt width, m. We calculated L as the ratio of shelterbelt area to cropland area (both values taken from land cover map as for the year 2021). We used K = 0.7 based on our expert knowledge of shelterbelts in eastern Ukraine. Most of these plantations have lacked necessary treatments and thus exhibit a dense aerodynamic construction.

We tested hypothesis H2 by comparing the calculated cropland protection function before the Russian invasion (2021) and for 2022 and 2023. We considered the mapped damaged pixels to correspond to degraded parts of shelterbelts and reduced the shelterbelt area accordingly. We calculated the average change in cropland protection function at the hexagonal and hromada levels.

2.5. Recommendations for regeneration

We mapped the detected damage to forest cover for the year 2023 to the forest types 'ravine protection plantations', 'shelterbelts', and 'roadside protective plantations' within specific soil types. For this step, we used a national-scale soil type map (based on soil investigations in 1957–1961, with local updates conducted in 1969–1991) in vector format. Pixel counts of the damaged forest cover mask were converted to area estimates. We used specific guidelines and scientific literature (Stadnik, 2018, Solomakha et al., 2022) to group soil types for assigning a recommended set of tree or shrub species for post-war regeneration. We used only the map of soil types as this combined indicator of soil fertility and humidity is the most important factor in deciding which species to plant (Dubyna et al., 2023). Our study area does not have specific climatic variability to be accounted for (Shvidenko et al., 2017). Additionally, we provided comments and suggestions on possible risks involving alien and invasive tree or shrub species for use in forest regeneration.

3. Results

3.1. Damage estimates and forest functional type mapping

We achieved moderate classification results with our rapid, semiautomated assessment of local forest types based on validation data (57 % of overall accuracy). While both water protection plantations and roadside protective plantations were distinguished with high precision and recall values (Table 2), other forest types were as successfully not delineated using raster patch characteristics. The majority of validation points for the class 'other' (unclassified forests) actually corresponded to shelterbelts (247 of 400), which explains the low recall value (38.4 %).

The total damage to forest cover in the study area is $92.4\pm26.1~\text{km}^2$ (11.5 %) in 2022 and $144.7\pm41.5~\text{km}^2$ (18.1 %) as of the year 2023 (Table 3), supporting our hypothesis H1. The growth in the estimated damaged forest cover was mainly attributed to 'low' damage, as depicted on delta NBR maps. For several forest types, there was even a decline in the estimated 'high damage' (e.g., for ravine protection plantations) in 2023 compared to the previous year, due to the spectral recovery of disturbed vegetation.

The detected 'high' damage to forest cover is unevenly distributed across administrative units (hromadas), if ravine and water protection plantations are considered (Fig. 3). These are concentrated between the towns Bakhmut and Lyman in the central part of the study area, the northern portion of Donetska oblast. Unlike these forest types, the damage to forest cover in shelterbelts, urban forests, and roadside protective plantations occurs evenly across the study area. However, Bakhmutska hromada exhibited the highest level of destruction as of September 2023 for all studied forest types, due to intense, continuous fighting since late autumn 2022.

3.2. Cropland protection function and recommendations for regeneration

We found that only ~ 2.7 % of the cropland protection function provided by shelterbelts has been lost at the study area level as of the end of 2023 (Fig. 4). This does not support our hypothesis H2, despite the progressive deterioration compared to 2022, when there was a 1.9 % loss in shelterbelt functionality. However, some local hotspots exhibit up to 57 % loss of this ecosystem function at the local (hexagonal) level. These hotspots are concentrated in specific parts of the study area and have clear links to the main battlefields of 2022 and 2023. In Kharkivska oblast (northern part of study area) these are areas south of the cities of Izium and Balakliia (target of the Russian offensive in summer 2022 towards the towns Sloviansk and Barvinkove) and at the border with Luhanska oblast (under Russian offensive since early 2023). In Donetska oblast, the main hotspots of the cropland protection functionality loss are around the cities of Vuhledar, Avdiivka and Bakhmut, the main local targets of the Russian offensive in the first two years of invasion.

The majority (81 %) of the detected damage as of 2023 in ravine protection plantations, shelterbelts, and roadside protective plantations has occurred on black earth soils, which can support a variety of native

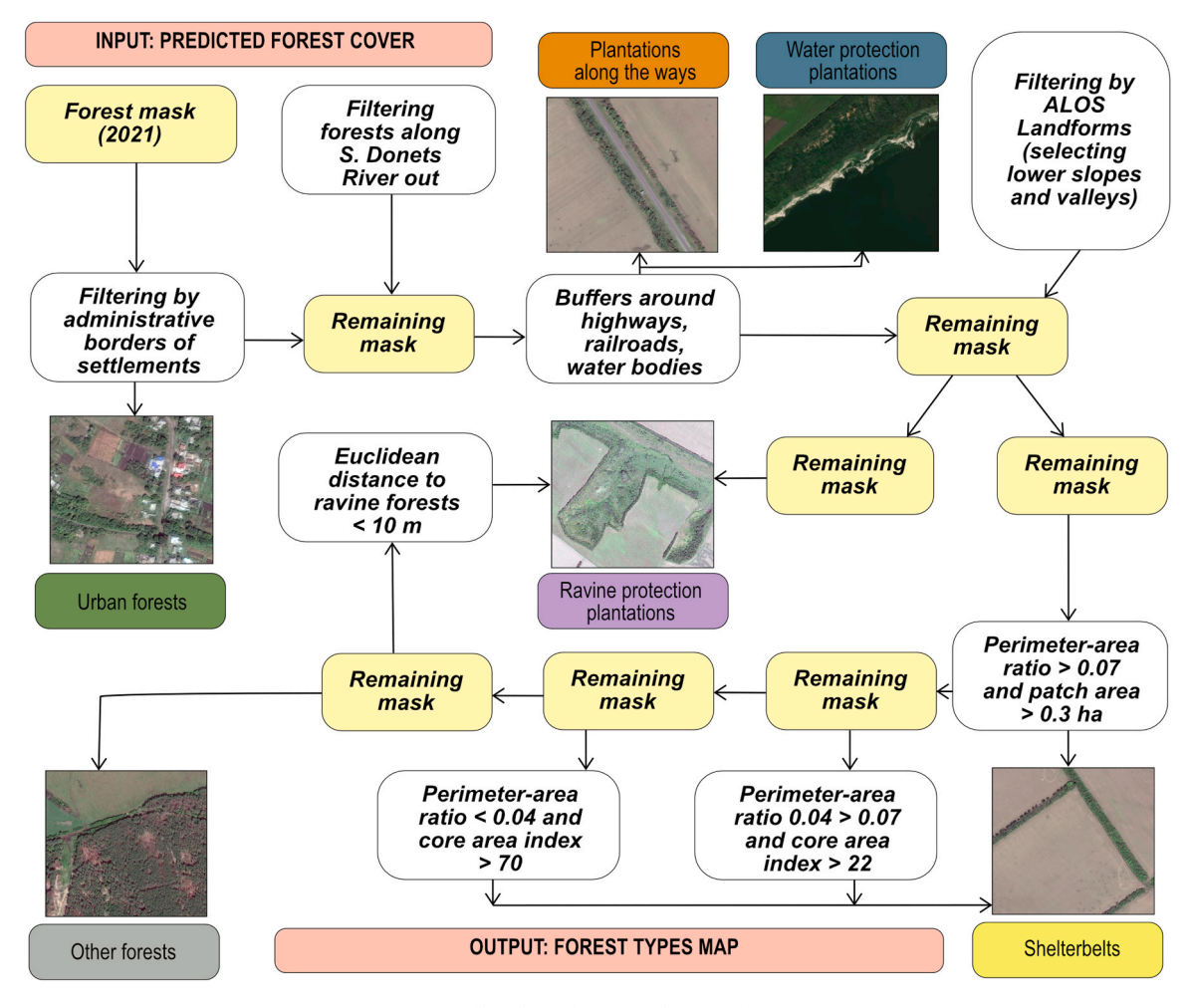


Fig. 2. Logical flowchart of creating the map of forest types.

Table 2
Confusion matrix and accuracy of the map of forest types.

Reference / Prediction	other forests	ravine protection	shelterbelts	water protection	roadside protective plantations
other forests	46	26	20	3	8
ravine protection	77	277	87	64	17
shelterbelts	247	39	235	5	86
water protection	21	50	28	326	16
roadside protective plantations	9	8	30	1	273
Precision, %	11.5	69.5	58.8	81.2	68.2
Recall, %	44.7	53.1	38.4	74.0	85.1

tree and shrub species for post-war regeneration (Table 4). In contrast, only 1.5 % of the damaged area for the specified forest functional types can be attributed to poor meadow solonetzic soils, which will be difficult to regenerate without introducing non-native tree and shrub species. Some risks in preferring alien species can be expected for the 10.3 % of damaged protective plantations located on gray and black podzolized soils.

Table 3Area estimates of damaged forest cover by forest types.

71	Area (2021),	Damage	Damaged forest cover area, km ²				Damaged cover, %	
	km²	low, 2022	low, 2023	high, 2022	high, 2023	2022	2023	
other forests	149.8	22.9	27.1	5.2	3.4	18.8	20.4	
		± 6.7	± 7.9	± 1.5	± 1.0			
ravine	243.6	14.4	36.5	3.2	2.4	7.2	16.0	
protection		± 3.9	± 9.8	± 0.9	± 0.7			
shelterbelts	151.0	19.8	28.4	4.1	4.1	15.8	21.5	
		± 5.8	± 8.4	± 1.2	± 1.2			
water	98.5	4.6	17.8	0.6	1.1	5.3	19.2	
protection		± 1.5	± 5.6	± 0.2	± 0.3			
roadside	79.4	8.7	16.3	1.7	2.5	13.1	23.7	
protective		± 2.6	± 4.9	± 0.5	± 0.7			
urban	76.2	5.9	0.5	1.3	4.5	8.4	18.7	
forests		± 1.2	± 0.1	± 0.3	± 0.9			

4. Discussion

4.1. Damage estimates and forest functional type mapping

We revealed that the levels of forest cover damage (as of 2023) in the eastern agroforestry region of Ukraine increased by 57 % compared to 2022, comprising 18 % of the 2021 cover (excluding the large forest massifs along the Siverskyi Donets River). This supports our hypothesis H1, which we tested using remote sensing data. Satellite imagery is a

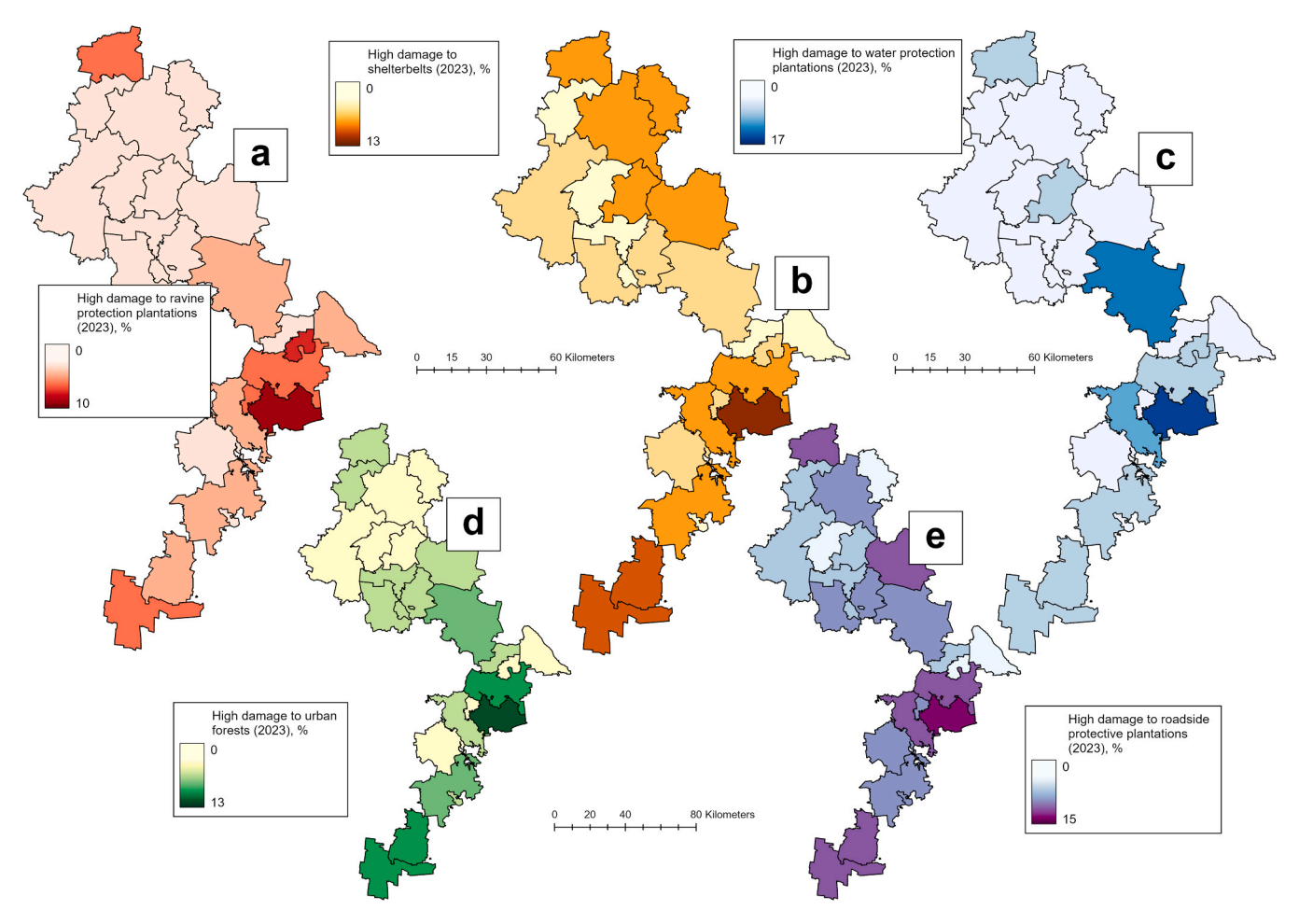


Fig. 3. Detected 'high' damage to studied forest types (as for 2023): ravine protection plantations (a); shelterbelts (b); water protection plantations (c); urban forests (d); roadside protective plantations (e).

suitable tool to assess forest loss and degradation related to military conflicts. Fires and tree harvest are the most common factors driving forest cover damage in conflict-affected regions, such as Ethiopia (Negash et al., 2023) and the Korean peninsula (Dong et al., 2020). Clear-cuts and high-severity fires can be easily detected by spectral changes in the infrared range of spectrum (Fig. 5a-b). This is a particular reason why researchers often focus on detecting forest cover loss (i.e., conversion to non-forest land cover, Butsic et al., 2015) rather than examining gradual degradation.

In our study, we derived estimates of damaged areas separately for categories of 'light' and 'high' severity using delta NBR maps. In the absence of field inspections or high-resolution airborne (including laser) scanning data, we should interpret the 'light' damage category with caution. High-resolution satellite data may not always be a reliable reference; for example, Fig. 5c depicts a shelterbelt clearly damaged by military vehicles, while Fig. 5d shows no visible damage, yet both plantations were mapped as 'lightly damaged'. These limitations of optical satellite imagery can also lead to misinterpretations of results. For instance, we detected a decrease in 'highly' damaged ravine protection plantations (Table 3) as of 2023 compared to 2022. We may assume that spectral recovery has occurred in these forests, similar to findings of Gorsevski et al. (2012) in conflict-affected South Sudan. However, spectral recovery, often with a major contribution by herbaceous and shrub species, does not equal functional recovery, especially when 'light' damage means mechanically broken trees and UXO contamination (Zibtsev et al., 2023).

Satellite data is, however, a superior reference tool for monitoring the long-term and often indirect impacts of armed conflicts. It can be used to detect not only forest degradation, but also tree cover gains (e.g., Negash et al., 2023). Time series-processing techniques have proven to be effective in distinguishing between natural disturbances (e.g., wildfires) and human disturbances (e.g., harvest) in war-affected areas (Matsala et al., 2024). A spatially explicit analysis of forest cover dynamics can be useful to uncover hidden patterns, such as those related to UXO contamination (Dong et al., 2020). According to our study, shelterbelts and other protective stands along the frontline with no detected damage can be mapped as areas with possible landmine contamination.

Instead of manually delimiting different forest functional types, we applied a rapid semi-automated classification based on available vector data and patch forest characteristics. We have achieved moderate results: in some areas, shelterbelts, ravine protection plantations and roadside protective trees were correctly mapped (Fig. 5e), while obvious errors still occur in other locations (Fig. 5d). The latter is apparently related to the coarse spatial resolution of available elevation data (90 m for the ALOS Landforms dataset) and the variety of shapes attributed to shelterbelts. Some shelterbelts, due to their pre-war degradation resulting from neglect, were mapped as discontinuous groups of pixels. A possible solution could be applying convolutional neural networks, a deep learning technique that accounts for both spectral and textural features of spatial objects and is successfully applied to mapping different land uses (e.g., Kussul et al., 2017). Another option can be to focus on the morphology of only one specific forest functional type: e.g., Deng et al. (2023) achieved almost 95 % accuracy for delineating shelterbelts from other forest cover.

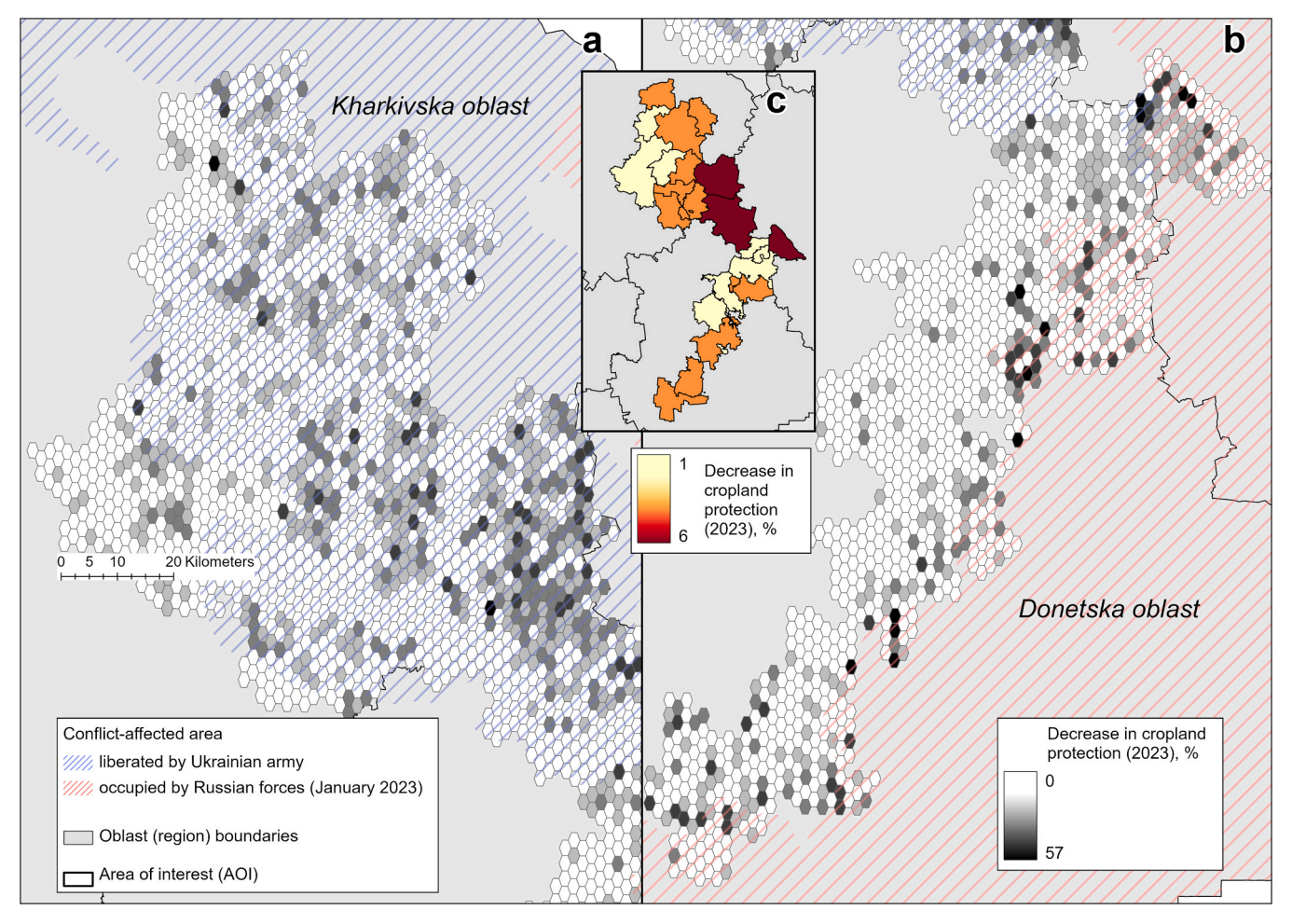


Fig. 4. Estimated loss in cropland protection function based on damage to shelterbelts (as for 2023): northern part of study area (a) and southern part of study area (b).

4.2. Cropland protection function and recommendations for regeneration

Although we detected an increase in loss of cropland protection function as of 2023 compared to 2022, this percentage is quite small – only 2.7 % on average across the study area. This can be explained by relatively minor damage to shelterbelts further away from the zone of active fights. Areas close to the frontline could exhibit up to 57 % deterioration in shelterbelt functionality, while landscapes located more than 50 km away from active battles were mostly unaffected. Consequently, we may assume that the rate of selective logging to harvest trees for building fortifications or for firewood supply to local communities, as well as fires caused by long-range projectiles (e.g., multiple launch rocket systems), is rather small in areas away from the frontline. However, agroforestry systems will also be threatened by damage to the croplands themselves (Skakun et al., 2019; Kussul et al., 2023).

Not all types of forest damage can be detected using medium-range satellite data, which in turn affects the accuracy of cropland protection function calculations. Even high-resolution remote sensing data may not be helpful in all cases (Fig. 5c-d), and certain war-related changes in shelterbelt functioning may go unaccounted for, potentially causing long-term negative impacts. Studies based on remote sensing data (e.g., Yang et al., 2021) can define shelterbelt functionality as windbreak efficiency at the landscape level, particularly in agroforestry systems with multiple fields. Simple detection of 'high' damage to certain pixels can guide adjustments to wind porosity from a horizontal perspective. However, changes in vertical structure may occur due to shelling and mechanical breakage of shelterbelt trees. On optical

satellite images, these damages may quickly be overshadowed by spectral recovery (due to the regrowth of herbs and shrubs), making efficient monitoring possible only through large-scale, preferably airborne, laser scanning.

We revealed that the majority (81 %) of damaged shelterbelts, ravine protection and roadside protective plantations can be attributed to black earth soils, the most fertile soil type in Ukraine. Unlike the southern part of Ukraine, which has partially saline lands suffering from frequent droughts, this finding leads to optimistic assumptions about the prioritized use of native tree and shrub species for regeneration (Dubyna et al., 2023). This is particularly relevant for the northern part of our study area, the forest-steppe ecozone in Kharkivska oblast, where European oak shelterbelts are considered the best option (Sydorenko and Sydorenko, 2018). However, it may also result in additional threats for sustainable recovery of agroforestry systems. First, financial difficulties in the immediate post-war period, combined with a focus on other pressing needs, may result in the rapid natural spread of alien species on such fertile soil before shelterbelts can be replanted. Second, establishing oak, poplar, and other traditional plantations will require long-term investments to maintain their optimal aerodynamic properties. For example, shelterbelts without timely silvicultural treatments become dense, while only a blown aerodynamic design provides the highest cropland protection functionality (Yukhnovskyi et al., 2020). Finally, there is a risk that alien species will be introduced for planting in ravines and degraded soils due to their high drought tolerance. This can lead to negative long-term effects: for instance, South Korea still faces challenges associated with the post-war practice of planting black locust for

Table 4Expected options for regeneration of damaged plantations by soil types (tree species).

Tree species	Soil types (area)						
	Black (9220 ha, 81.0 %)	Gray and black podzolized (1169 ha, 10.3 %)	Black with carbonates (626 ha, 5.5 %)	Podzolized (198 ha, 1.7 %)	Meadow solonetzic (172, 1.5 %)		
Pinus sylvestris L.			✓	√			
Quercus robur L.	✓	✓		✓			
Betula pendula Roth.	✓	✓		✓			
Larix sibirica Ledeb.				✓			
Pinus nigra subsp.				✓			
pallasiana							
Robinia pseudoacacia L.	✓	✓	✓	✓			
Alnus glutinosa				✓			
(Gaertn.) L.							
Fraxinus excelsior L.	✓	✓		✓			
Gleditsia triacanthos L.	✓				✓		
Juglans regia L.	✓						
Juglans nigra L.	✓						
Populus spp.	✓						
Salix alba L.	✓						
Ulmus parvifolia Jacq.	✓				/		
Armeniaca vulgaris L.	✓	✓					
Acer platanoides L.	✓	✓	✓				
Acer campestre L.	✓	✓			✓		
Carpinus betulus L.	✓	✓					
Fraxinus pennsylvanica Marshall	1						
Malus domestica Borkh.	✓	✓					
Morus alba L.	✓	✓					
Padus serotina Ehrh.	✓	✓					
Prunus avium L.	✓		✓		✓		
Pyrus communis L.	✓						
Tilia cordata L.	✓	✓	✓				
Ulmus minor Mill.	✓	✓					
Acer tataricum L.	✓	✓			✓		
Juniperus virginiana L.			✓				
Styphnolobium japonicum	ı (L.) Schott		✓				
Fraxinus oxycarpa Bieb. e	x Willd.				✓		
Alnus incana (L.)		✓					
Moench							

erosion control and fuel supply (Martin, 2023). So far, Ukrainian legislation has been ambiguous regarding species selection for forest regeneration: for timber production, Scots pine or European oak must always be prioritized, but alien species have not been explicitly prohibited. Recent attempts to change it have led to tense discussions between policymakers, researchers, forest practitioners, and farmer representatives (Dubyna et al., 2023).

Our approach with spatially analyzing possible niches for post-war regeneration has several limitations. We used a soil type map with coarse resolution due to absence of more accurate spatially explicit data. While digital terrain models (DTM) can be used to remotely approximate different soil properties (Agren et al., 2021), there is no high-resolution DTM available for the whole region of eastern Ukraine. Field inspections can provide the necessary information about succession processes in shelterbelts at different levels of war-related damage. However, for security reasons, such a data collection campaign can only take place in hromadas of Kharkivska oblasts liberated in 2022. The list of such areas will be even more limited by proximity to the current frontline and UXO contamination.

5. Conclusions

We revealed that 18 % of forest plantations in the east of Ukraine were damaged due to Russian invasion as of 2023. These forests, excluding the large massifs along the Siverskyi Donets River, are mainly designed to control erosion, regulate water supply, and protect agricultural systems. Our hypothesis regarding increasing deterioration compared to 2022 due to intensifying battles was supported by our remote sensing data, but we did not observe a significant drop in cropland protection function at the regional scale. While several areas in

proximity to the frontline exhibit the loss of this ecosystem function up to $57\,\%$, the majority of shelterbelts across the studied administrative units remain largely untouched.

We are optimistic that the majority (81 %) of the detected damage occurred on fertile black earth soils, which should allow for easy regeneration with native species. However, the success of this trajectory will depend on financial priorities and legislative clarity. We also highlight the limitations of relying solely on satellite data analysis, as airborne laser scanning and field inspections are necessary to gain a deeper understanding of war-related impacts on protective plantations.

CRediT authorship contribution statement

Serhii Sydorenko: Writing – review & editing, Software, Methodology, Investigation, Formal analysis, Data curation. Svitlana Sydorenko: Writing – review & editing, Validation, Methodology, Investigation, Data curation. Maksym Matsala: Writing – review & editing, Writing – original draft, Visualization, Validation, Supervision, Software, Project administration, Methodology, Investigation, Formal analysis, Data curation, Conceptualization. Andrii Odruzhenko: Software, Investigation, Formal analysis, Data curation.

Declaration of Competing Interest

The authors declare that they have no known competing financial interests or personal relationships that could have appeared to influence the work reported in this paper, Andrii Odruzhenko reports financial support was provided by Ministry of Education and Science of Ukraine. If there are other authors, they declare that they have no known competing financial interests or personal relationships that could have

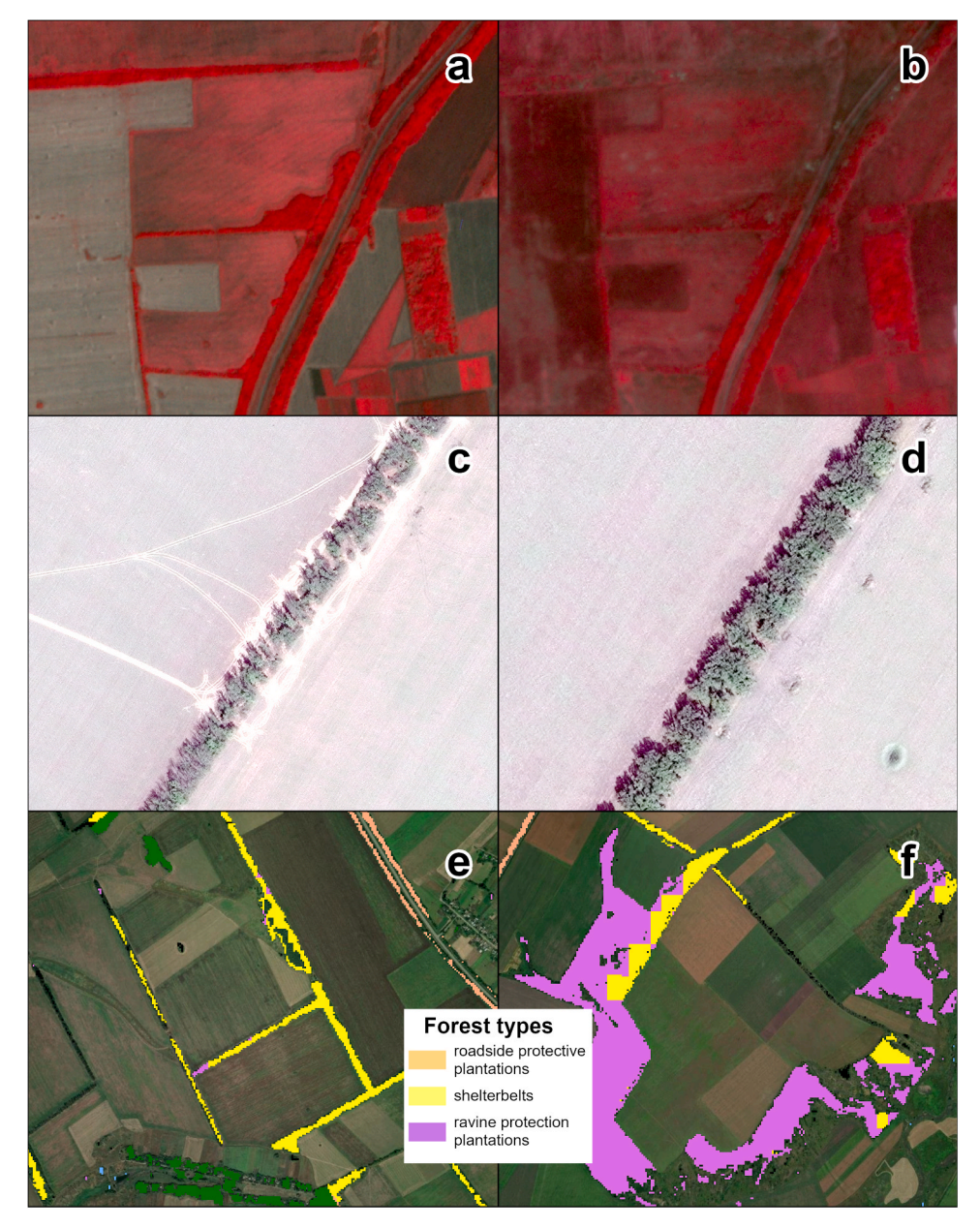


Fig. 5. Example of false-color (Near Infrared - Red - Green) imagery from the Planet satellite (3 m resolution) depicting agroforestry system to the south of Bakhmut before the Russian invasion (a) and in 2023 (b); shelterbelts illustrated in true-color imagery from the World-View satellite (40 cm resolution) to the north of Izium, with (c) and without (d) clearly visible mechanical damage; correctly (e) and incorrectly (f) mapped forest functional types in Kharkivska oblast.

appeared to influence the work reported in this paper.

Acknowledgements

Study was partially supported by Ministry of Education and Science of Ukraine (grant number #110/3m-pr-2022) and by MSCA4Ukraine

under grant agreement No. 1233687 for project "Ukrainian wildfires of war: changes in fire regimes as a result of the direct and indirect effects of war". We are grateful to Tetyana Kuchma for her valuable comments and suggestions and to Brian Milakovsky for language editing support. We are grateful to all defenders of Ukraine for allowing us to continue our research.

Appendix

Table A1Expected options for regeneration of damaged plantations by soil types (shrub species)

Tree species	Soil types (area)						
	Black (9220 ha, 81.0 %)	Gray and black podzolized (1169 ha, 10.3 %)	Black with carbonates (626 ha, 5.5 %)	Podzolized (198 ha, 1.7 %)	Meadow solonetzic (172, 1.5 %)		
Amorpha fruticosa L.				✓			
Rosa canina L.			✓	✓			
Amelanchier ovalis Medik.	✓		✓		✓		
Caragana arborescens Lam.	✓	✓	✓		✓		
Chaenomeles japonica (Thunb.)	✓	✓					
Lindl. ex Spach							
Corylus avellana L.	✓						
Cotinus coggygria Scop.	✓		✓				
Cotoneaster lucidus Schltdl.	✓	✓					
Elaeagnus angustifolia L.	✓	✓	✓	✓	✓		
Hippophae rhamnoides L.	✓	✓					
Ligustrum vulgare L.	✓						
Mahonia aquifolium Pursh	✓		✓		✓		
Ribes aureum Pursh	✓				✓		
Lonicera tatarica L.					✓		
Tamarix spp.					✓		
Crataegus monogyna Jacq.		✓					

Note. Alien shrub species are marked by orange color.

Data Availability

Data will be made available on request.

References

- Agren, A.M., Larson, J., Shekhar Paul, S., Laudon, H., Lidberg, W., 2021. Use of multiple LIDAR-derived digital terrain indices and machine learning for high-resolution national-scale soil moisture mapping of the Swedish forest landscape. Geoderma 404, 115280, https://doi.org/10.1016/j.geoderma.2021.115280.
- Bey, A., Sanchez-Paus Diaz, A., Maniatis, D., Miceli, G., 2016. Collect earth: land use and land cover assessment through augmented visual interpretation. Remote Sens. 8 (10), 807. https://doi.org/10.3390/rs8100807.
- Butsic, V., Baumann, M., Shortland, A., Walker, S., Kuemmerle, T., 2015. Conservation and conflict in the democratic Republic of Congo: the impacts of warfare, mining, and protected areas on deforestation. Biol. Conserv. 191, 266–273. https://doi.org/ 10.1016/j.biocon.2015.06.037.
- Deng, R., Guo, Q., Jia, M., Wu, Y., Zhou, Q., Xu, Z., 2023. Extraction of farmland shelterbelts from remote sensing imagery based on a belt-oriented method. Front. For. Glob. Change 6, 1247032. https://doi.org/10.3389/ffgc.2023.1247032.
- Depountis, N., Michalopoulou, M., Kavoura, K., Nikolakopoulos, K., Sabatakakis, N., 2020. Estimating soil erosion rate changes in areas affected by wildfires. Int. J. Geo-Inf. 9 (10), 562. https://doi.org/10.3390/ijgi9100562.
- Dong, Y., Ren, Z., Wang, Z., Yu, Q., Zhu, L., Yu, H., Bao, G., 2020. Spatiotemporal patterns of forest changes in korean peninsula using landsat images during 1990–2015: a comparative study of two neighboring Countries. IEEE Access 8, 73623–73633. https://doi.org/10.1109/ACCESS.2020.2988122.
- Dubyna, D.V., Ustymenko, P.M., Baranovski, B.A., Karmyzova, L.A., 2023. Forest strips of Ukraine in the modern realities, state assessment and ways of their restoration. Agrology 6 (2), 38-44. https://doi.org/10.32819/021205.
- Yukhnovskyi, V., Polishchuk, O., Lobchenko, G., Khryk, V., Levandovska, S., 2020. Aerodynamic properties of windbreaks of various designs formed by thinning in central Ukraine. Agrofor. Syst. 95, 855–865. https://doi.org/10.1007/s10457-020-00503-8.
- Forest Code (2006). $\langle https://zakon.rada.gov.ua/laws/show/3852-12\#Text \rangle$ (in Ukrainian).
- Gleick, P., Vyshnevskyi, V., Shevchuk, S., 2023. Rivers and water systems as weapons and casualties of the Russia-Ukraine War. e2023EF003910 Earth'S. Future 11. https://doi.org/10.1029/2023EF003910.
- Gorelick, N., Hancher, M., Dixon, M., Ilyushchenko, S., Thau, D., Moore, R., 2017. Google Earth engine: planetary-scale geospatial analysis for everyone. Remote Sens. Environ. 202, 18–27.
- Gorsevski, V., Kasischke, E., Dempewolf, J., Loboda, T., Grossmann, F., 2012. Analysis of the impacts of armed conflict on the Eastern Afromontane forest region on the South Sudan — Uganda border using multitemporal Landsat imagery. Remote Sens. Environ. 118, 10–20. https://doi.org/10.1016/j.rse.2011.10.023.
- Hall, J.V., Zibtsev, S.V., Giglio, L., Skakun, S., Myroniuk, V., Zhuravel, O., Goldammer, J. G., Kussul, N., 2021. Environmental and political implications of underestimated cropland burning in Ukraine. Environ. Res. Lett. 16, 064019. https://doi.org/10.1088/1748-9326/abfc04.

- Kussul, N., Drozd, S., Yailymova, H., Shelestov, A., Lemoine, G., Deininger, K., 2023. Assessing damage to agricultural fields from military actions in Ukraine: an integrated approach using statistical indicators and machine learning. Int. J. Appl. Earth Obs. Geoinf. 125, 103562. https://doi.org/10.1016/j.jag.2023.103562.
 Kussul, N., Lavreniuk, M., Skakun, S., Shelestov, A., 2017. Deep Learning Classification
- Kussul, N., Lavreniuk, M., Skakun, S., Shelestov, A., 2017. Deep Learning Classification of Land Cover and Crop Types Using Remote Sensing Data. IEEE Geosci. Remote Sens. Lett. 14 (5), 778–782. https://doi.org/10.1109/LGRS.2017.2681128.
- Martin, A., 2023. Factors influencing the use of introduced black locust (Robinia pseudoacacia) for slope stabilization in post-war South Korea. Trees, For. People 14, 100444. https://doi.org/10.1016/j.tfp.2023.100444.
- Matsala, M., Odruzhenko, A., Hinchul, T., Myroniuk, V., Drobyshev, I., Sydorenko, S., Zibtsev, S., Milakovsky, B., Schepaschenko, D., Kraxner, F., Bilous, A., 2024. War drives forest fire risks and highlights the need for more ecologically-sound forest management in post-war Ukraine. Sci. Rep. 14, 4131. https://doi.org/10.1038/ s41598-024-54811-5.
- Myroniuk, V., Kutia, M., Sarkissian, A.J., Bilous, A., Liu, S., 2020. Regional-scale forest mapping over fragmented landscapes using global forest products and Landsat time series classification. Remote Sens. 12, 187. https://doi.org/10.3390/rs12010187.
- Negash, E., Birhane, E., Gebrekirstos, A., Nyssen, J., 2023. Remote sensing reveals how armed conflict regressed woody vegetation cover and ecosystem restoration efforts in Tigray (Ethiopia). Sci. Remote Sens. 8, 100108. https://doi.org/10.1016/j. srs.2023.100108
- Nowak, M.M., Pedziwiatr, K., Bogawski, P., 2022. Hidden gaps under the canopy: LiDAR-based detection and quantification of porosity in tree belts. Ecol. Indic. 142, 109243. https://doi.org/10.1016/j.ecolind.2022.109243.
- Olofsson, P., Foody, G.M., Herold, M., Stehman, S.V., Woodcock, C.E., Wulder, M.A., 2014. Good practices for estimating area and assessing accuracy of land change. Remote Sens. Environ. 148, 42–57. https://doi.org/10.1016/j.rse.2014.02.015.
- Pereira, P., Basic, F., Bogunovic, I., Barcelo, D., 2022. Russian-Ukrainian war impacts the total environment. Sci. Total Environ. 837, 155865. https://doi.org/10.1016/j.ccitcotany.2022.155865
- Rawtani, D., Gupta, G., Khatri, N., Rao, P.K., Hussain, C.M., 2022. Environmental damages due to war in Ukraine: a perspective. Sci. Total Environ. 850, 157932. https://doi.org/10.1016/j.scitotenv.2022.157932.
- Shevchuk, S.A., Vyshnevskyi, V.I., Bilous, O.P., 2022. The use of remote sensing data for investigation of environmental consequences of Russia-Ukraine war. J. Landsc. Ecol. 15 (3), 36–53. https://doi.org/10.2478/jlecol-2022-0017.
- Shumilo, L., Skakun, S., Gore, M.L., Shelestov, A., Kussul, N., Hurtt, G., Karabchuk, D., Yarotskiy, V., 2024. Conservation policies and management in the Ukrainian Emerald Network have maintained reforestation rate despite the war. Commun. Earth Environ. 4, 443. https://doi.org/10.1038/s43247-023-01099-4.
- Shumilova, O., Tockner, K., Sukhodolov, A., Gleick, P., 2023. Impact of the Russia–Ukraine armed conflict on water resources and water infrastructure. Nat. Sustain. 6, 576–586. https://doi.org/10.1038/s41893-023-01068-x.
- Shvidenko, A., Buksha, I., Krakovska, S., Lakyda, P., 2017. Vulnerability of Ukrainian forests to climate change. Sustainability 9 (7), 1152.
- Skakun, S., Justice, C.O., Kussul, N., Shelestov, A., Lavreniuk, M., 2019. Satellite data reveal cropland losses in south-eastern Ukraine under military conflict. Front. Earth Sci. 7, 305. https://doi.org/10.3389/feart.2019.00305.
- Solomakha, I., Sabluk, V., Gumentyk, M., Solomakha, V., 2022. Features of creating fast-growing and multifunctional field-protecting forest strips in the forest-steppe zone of

- Ukraine. Agroecol. J. (4), 6–15. https://doi.org/10.33730/2077-
- Soshenskyi, O., Myroniuk, V., Zibtsev, S., Gumeniuk, V., Laschchenko, A., 2022. Evaluation of field-based burn indices for assessing forest fire severity in Luhansk Region, Ukraine. Ukr. J. For. Wood Sci. 13 (1), 48–57. https://doi.org/10.31548/ forest.13(1).2022.48-57.
- Stadnik A. (2018). Optimization of the structure of protective forest plantations and their systems in agricultural landscapes of Ukraine. Proceedings of the Forestry Academy of Sciences of Ukraine, (16), 70-80. https://doi.org/10.15421/411808 (in Ukrainian).
- Sun, Q., Zheng, B., Liu, T., Zhu, L., Hao, Z., Han, Z., 2022. The optimal spacing interval between principal shelterbelts of the farm-shelter forest network. Environ. Sci. Pollut. Res. 29, 12680–12693. https://doi.org/10.1007/s11356-021-17272-1.
- Sydorenko, S.V., Sydorenko, S.H., 2018. Current status and growth of shelterbelts in the Kharkiv region and their meliorative efficiency. For. For. Melior. (133), 39–53. https://doi.org/10.33220/1026-3365.133.2018.39.
- Sydorenko, S., Voron, V., Koval, I., Sydorenko, S., Rumiantsev, M., Hurzhii, R., 2021. Postfire tree mortality and fire resistance patterns in pine forests of Ukraine. Cent. Eur. For. J. 67, 21–29. https://doi.org/10.2478/forj-2020-0029.
- Vacek, Z., Rehacek, D., Cukor, J., Papaj, V., 2018. Windbreak efficiency in agricultural landscape of the central Europe: multiple approaches to wind erosion control. Environ. Manag. 62, 942–954. https://doi.org/10.1007/s00267-018-1090-x.
- Yang, X., Li, F., Fan, W., Liu, G., Yu, Y., 2021. Evaluating the efficiency of wind protection by windbreaks based on remote sensing and geographic information systems. Agrofor. Syst. 95, 353–365. https://doi.org/10.1007/s10457-021-00594-x.
- Zibtsev S., Soshenskyi O., Goldammer J.G., Myroniuk V., Borsuk O., Gumeniuk V., Mieshkova V., Vasyliuk O., Buksha I. (2023). Forest management on territories contaminated with unexploded ordnance. Technical report, WWF-Ukraine.